Check for updates

Synergistic cyclic cooperativity governs the strength of chalcogen, pnictogen and tetrel bonds in microhydrated clusters†

Ayush Shivhare, [ID] [a] Chandan Kumar Lenka, [ID] [a] Bharti Dehariya [ID] [a] and Milind M. Deshmukh [ID] *[b]

It has been demonstrated that the sum of the cooperativity contributions (CCs) of the cyclic structures (common to a referenced hydrogen bond (HB)) when added to the energy of the HB in the respective dimer provides an accurate estimation of its energy in an actual molecular cluster. For this purpose, a molecular tailoring approach (MTA)-based method was utilized to estimate the CCs of these cycles. The HB energies calculated in this fashion ($E_{HB}^{Synergetic}$) were in excellent agreement with those of their actual cluster counterparts ($E_{HB}^{Cluster}$). In this study, the generality of this methodology for estimating the energy of other non-covalent bonds (NCBs), *viz.* tetrel (TBs), chalcogen (CBs) and pnictogen bonds (PBs), in microhydrated clusters is tested. For this purpose, the microhydrated clusters of carbon dioxide (CO_2), nitrous (N_2O) oxide and sulphur dioxide (SO_2) are employed. These microhydrated clusters exhibit TBs, PBs and CBs with the surrounding water molecules. The energies of these NCBs calculated using the synergetic cyclic cooperativity ($E_{NCB}^{Synergetic}$) approach were found to be in excellent agreement with those of their full cluster counterparts ($E_{NCB}^{Cluster}$) calculated using the MTA-based method. The difference between the two values was found to be less than 0.6 kcal mol^{-1}. It is emphasized here that the variation in the strength of these different NCBs can be nicely explained in terms of the interplay of the nature of the cooperativity exhibited by the cyclic structures common to them.

Introduction

For the past two decades, there has been growing interest in exploring the understanding of non-covalent bonds (NCBs) other than the hydrogen bonds (HBs).[1–8] Among these, halogen bonding (XB) has been quite extensively explored.[1] In addition, pnictogen (PB), chalcogen (CBs) and tetrel bonds (TBs) have recently attracted significant attention.[2–7] Molecular electrostatic potential (MESP) analysis is often used in interaction studies to recognize the preferential sites of donors and acceptors.[8–10] These terminologies (TB, PB and CB) comprise the atoms of groups 14, 15 and 16 of a molecule, in which a positive electrostatic potential (MESP) is often found to interact with the suitable electron donor species. Depending on the position of positive MESP to be along or perpendicular to the molecular plane, the concepts of σ and π-holes have been used.[11,12] Although research on these NCB

[a] Department of Chemistry, Dr Harisingh Gour Vishwavidyalaya (A Central University), Sagar 470003, India. E-mail: ayushshivharepanna@gmail.com, chandankumarlenka80@gmail.com, dehariyabharti29@gmail.com

[b] Department of Chemistry, University of Delhi, 110007, Delhi, India. E-mail: milind.deshmukh@gmail.com, mdeshmukh@dhsgsu.edu.in

† Electronic supplementary information (ESI) available: Molecular energies (in a.u.) of various species of **TB1** energy evaluation in cyclic trimers **a** and **b** of **CW3B** cluster using the MTA-based method in Tables S1 and S2, respectively; molecular energies (in a.u.) of various species of **TB1** energy evaluation in the actual **CW3B** cluster by the MTA-based method in Table S3; representation of a PB and CB in cyclic trimers in Schemes S1 and S2; The MP2/aug-cc-pVDZ geometry of CW3B clusters exhibiting a TB common to two cyclic structures (a) and (b), both exhibiting full cyclic cooperativity in Scheme S3. The fragmentation procedure of the MTA-based method for calculating the energy of **TB1** in the cyclic trimer **b** of CW3B cluster in Scheme S4; the fragmentation procedure of the MTA-based method for calculating the energy of **TB1** in CW3B cluster in Scheme S5; the structure of the $CO_2(H_2O)_n$ clusters showing different types of cyclic structures exhibiting FCC, PCC or AC towards TBs common to these cycles in Scheme S6; the fragmentation procedure of MTA-based method for calculating the energy of **PB1** in cyclic trimers **a** and **b** of **NW3C** clusters in Schemes S7 and S8; the fragmentation procedure of MTA-based method for calculating the energy of **PB1** in the **NW3C** cluster in Scheme S9. Optimized geometries of lowest energy conformers of $N_2O(H_2O)_3$ in Scheme S10; the structure of the $N_2O(H_2O)_n$ clusters showing different types of cyclic structures exhibiting FCC, PCC or AC towards PBs in Scheme S11; the fragmentation procedure of MTA-based method for calculating the energy of **CB1** in the cyclic trimers **a** and **b** of **SW3A** cluster in Schemes S12 and S13; the fragmentation procedure of MTA-based method for calculating the energy of **CB1** in the **SW3A** cluster in Scheme S14; and the structure of the $SO_2(H_2O)_n$ clusters showing different types of cyclic structures exhibiting FCC, PCC or AC towards CBs in Scheme S15. See DOI: https://doi.org/10.1039/d5cp02070k

15960 | *Phys. Chem. Chem. Phys.*, 2025, **27**, 15960–15974

This journal is © the Owner Societies 2025

complexes involving TB, PB and CB is increasing daily, it is limited to the study of the interaction present in the dimeric complex. There are few examples reported recently wherein the effect of a third molecule on the strength of these NCBs has been investigated.[13–15] The presence of a third molecule either enhances or diminishes the strength of a referenced NCB.[16] The enchantment or decrement in the strength of a referenced NCB due to the presence of surrounding molecules is called cooperativity or anti-cooperativity, respectively.

Cooperativity is an important feature in modulating the strength of NCBs. This phenomenon is popular and recognized in the context of HBs. For instance, the cooperativity corresponding to the interconnected networks of HBs has been extensively studied in molecular clusters of water $(H_2O)_n$,[17] hydrogen fluoride $(HF)_n$,[18] and ammonia $(NH_3)_n$[19] as well as in intramolecular hydrogen-bonded systems.[20,21] The HB cooperativity is found to be responsible for the properties of liquids,[22,23] hydration of ions,[24,25] and the structure of large supramolecular aggregates and biomolecules.[26,27] Cooperativity is observed when the direction of all the HBs (donor to acceptor) is same either in a linear or cyclic structure; such a cycle is called a homodromic cycle. However, anti-cooperativity prevails when this directionality is broken at two or more neighboring HBs, resulting in the formation of an antidromic cycle.[28] It has been reported that a large three-dimensional (3D) structure of a molecular cluster is made up of small cyclic structures with a different number of HBs.[29] The cooperativity and anti-cooperativity of these homodromic or antidromic cycles are crucial to determine the strength of the HBs, which are present at the interface of these cyclic structures. However, the methods available in the literature[30–38] cannot be employed to understand the individual HB energy and cooperativity contribution of neighboring molecules towards them in molecular clusters. To understand the nature of cooperativity in a given 3D molecular cluster, the quantitative estimates of the individual HB strength and the cooperativity contribution of other HBs towards them are essential.

With this understanding, Deshmukh and Gadre developed a molecular tailoring approach (MTA)-based method for direct, reliable estimation of the energy of individual HBs in various molecules,[38–44] molecular clusters[45–49] and crystals.[50] In a large 3D molecular cluster, it has been found that an HB may be present at the intersection of two or more cyclic structures of the interconnected HB networks.[29] Shivhare and Deshmukh demonstrated that the energy of such an X–H···Y HB in molecular clusters can be accurately determined in terms of cooperativity contributions (CCs) of these cyclic structures.[51,52] For instance, the MTA-based method was employed to calculate the CCs of these individual cycles. The CCs of all these cyclic structures were added to the energy of this HB in the corresponding dimer chopped out of the 3D molecular cluster.[51,52] The energy of an HB calculated in this manner (in terms of synergetic effects of the cooperativity of cyclic structures) is denoted by $E_{HB}^{Synergetic}$. The $E_{HB}^{Synergetic}$ values were found to be in excellent agreement with their full calculation counterparts obtained by applying the MTA-based method using the actual cluster.

It is emphasized here that there are only few investigations reported in the literature directed towards the understanding of the cooperativity effect on the strength of TBs, PBs and CBs along with HBs. For instance, one of the early studies investigated a ring-shaped molecular complex formed by CH_3, COX_2 or CSX_2 (X = F, Cl) and HY (Y = CN, NC), which are connected via two HBs and a single TB.[53] It was concluded that the contribution of three-body terms (measure of cooperativity) to the total interaction energy significantly depends on the nature of the substituents (X and Y), which is largest and smallest for the CH_3···CSF_2···HNC and CH_3···$CSCl_2$···HNC complexes, respectively.[53] Another interesting study was conducted by Li and coworkers[54] who investigated the ternary complexes of $PhTY_3$···4-X-pyridine···N-base (N-base = HCN, NH_3, $NHNH_2$, and NH_2CH_3; T = C, Si, and Ge; Y = H, F and Cl; and X = bromo or iodo).[54] The 4-Halopyridine with σ-hole on the halogen atom leads to the formation of halogen bond (XB), while the electron-deficient tetrel (T) atom in $PhTY_3$ is involved in the formation of a TB. The strengths of both XBs and TBs are reported to be enhanced owing to positive cooperativity, whereas the strengths of both HB and XB in $PhCF_3$···4-iodopyridine···NH_3 are weakened as a result of negative cooperativity.[54] A similar study involving F^-···$(CH_3)_2X$···YF (X = O, S, Se; Y = F, H) triads was reported by McDowell,[55] wherein a significant enhancement of the X···Y interactions relative to the neutral $(CH_3)_2X$···YF dyads was reported. Scheiner and coworkers[13] also performed ab initio calculations of dimers and trimers formed by imidazole (IM) and F_2TO (T = C, Si, Ge) molecules. A certain trimeric complex with negative cooperative TB between the central F_2TO molecule and two IM molecules was reported. The total interaction energy of the ternary complex is smaller than the sum of the two separate TBs in the IM···F_2TO dimer. Alternate configurational geometries stabilized by positive cooperativity was also reported in which the second IM formed an HB through the NH group of the first IM. The formation of such a positive cooperative ternary complex is also reflected in terms of shorter intermolecular distances. Deshmukh and coworkers investigated the geometries and NCB energies in microhydrated complexes of nitric oxide (NO).[56] It was found that neutral NO can form HB and PBs with water depending on the orientation; however, such HBs and PBs are weaker compared to the water···water HBs. This was attributed a smaller value of cooperativity contributions (−0.66 to 1.31 kcal mol^{-1}) found for NO···water and a moderate cooperativity contribution for water···water HBs (−0.20 to 4.38 kcal mol^{-1}). However, NO$^+$ species form stronger PBs with significant positive cooperativity contributions (5.08 to 17.84 kcal mol^{-1}). The strength of water···water HBs in NO$^+$ microhydrated clusters was weak owing to significantly negative cooperativity contributions (−0.05 to −1.69 kcal mol^{-1}).

In summary, although the studies reported in the literature are useful to understand the cooperative effect of neighboring molecules on the strength of other NCBs (such as TBs, PBs and CBs), a thorough investigation to modulate the effect of homodromic (cooperative) and antidromic (anti-cooperative) cooperative cycles involving TBs, PBs and CBs along with HBs in

microhydrated clusters is indispensable. Important questions to be answered here are as follows: (i) whether the synergetic cyclic cooperativity effect investigated earlier in the context of HBs is also applicable to TBs, PBs and CBs or not? (ii) In other words, is synergetic cyclic cooperativity a general phenomenon? and (iii) Is it possible to accurately determine the energies of these NCBs (other than HBs) in terms of synergetic cooperativity effects of cyclic structures to which they are common? To answer these important questions, in this study, the microhydrated clusters of carbon dioxide (CO_2), nitrous oxide (N_2O) and sulphur dioxide (SO_2) are investigated. The primary focus of the present investigation is to study these TBs, PBs and CBs, which are at the interface of two or more cyclic structures formed by the interconnected NCBs between CO_2, N_2O and SO_2 molecules and water molecules in their microhydrated clusters.

Method and computational details

The geometries of microhydrated clusters *viz.* $(CO_2)(H_2O)_n$, $(N_2O)(H_2O)_n$, and $(SO_2)(H_2O)_n$ with n = 1, 5 water molecules were optimized at the MP2/6-311++G(d,p) level of theory. Frequency calculations were performed at the same level of theory to confirm the local minimum nature of the optimized structures. Single point (SP) energy calculations at the MP2/aug-cc-pVTZ level is performed on the optimized structures and their fragments of the MTA-based method. The SP energies are then used to calculate the energies and CCs to TB, PB and CBs in these microhydrated clusters. All the calculations were carried out using the Gaussian 16 package.[57]

Results and discussion

Types of cyclic cooperativity experienced by non-covalent bonds

To characterize the direction of flow of electron density from nucleophile to electron-deficient atoms of groups 14 (tetrels), 15 (pnictogens) and 16 (chalcogens), the molecular electrostatic potential (MESP) is useful. Fig. 1 illustrates the MESP mapped on the iso-density surface (value = 0.001 a.u.) along with the respective values of the MESP surface minima (V_{min}) and
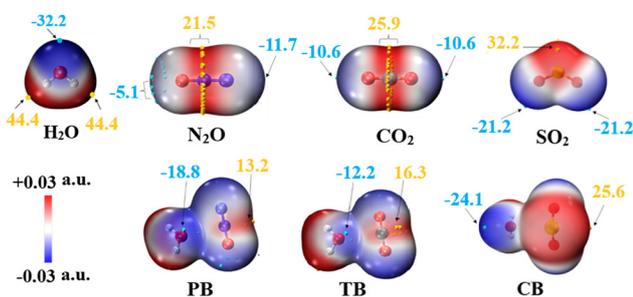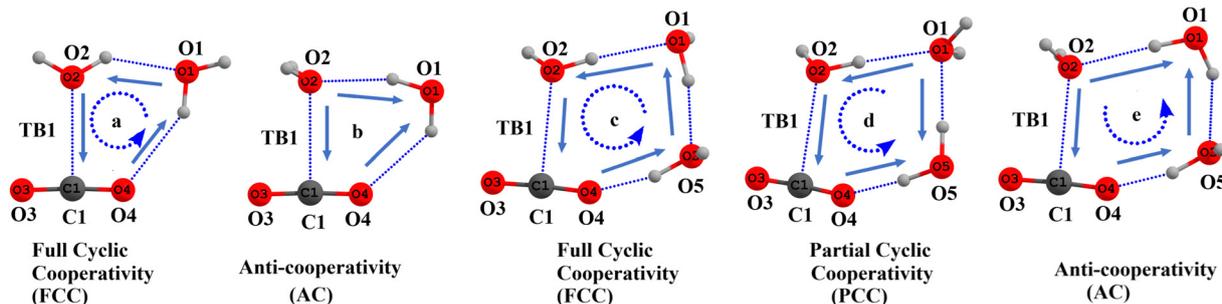

Fig. 1 Electrostatic potential mapped on the iso-density molecular surface (at 0.001 a.u.) for various monomers and their dimeric complexes with water. The positions of V_{min} and V_{max} at the interacting sites are represented by cyan and golden spheres, respectively, with the corresponding values in kcal mol^{-1}. Color ranges: blue indicates negative potential and red indicates positive potential.

maxima (V_{max}) for various monomers and their respective dimeric complexes.

The positions of these V_{min} and V_{max} values correspond to the site's electrophilic and nucleophilic attack, respectively. The electron-deficient regions on the tetrel (carbon), pnictogen (nitrogen) and chalcogen (sulphur) atoms are clearly evident from the appearance of surface maximum around the region perpendicular to the N_2O (V_{max} = 21.5 kcal mol^{-1}) or CO_2 (V_{max} = 25.9 kcal mol^{-1}) bond axis. Additionally, in the case of SO_2 (V_{max} = 32.3 kcal mol^{-1}), it is observed over the S-atom. However, in the H_2O molecule, the surface minima appear around the oxygen atom (V_{min} = −32.2 kcal mol^{-1}). For other molecules, it appears near the terminal hetero (N or S) atoms. Upon complex formation, the V_{min} value on the O-atom of the water molecule is substantially increased (becoming less negative) in all the dimeric complexes. This is nicely complemented by the decrease (becoming less positive) in V_{max} values, indicating the transfer of electron density from the water molecule to the counter-molecule, which establishes the NCBs, *viz.* PB, TB or CB.

With this understanding, one can identify the nature of the cyclic structure that may be observed in the microhydrated clusters of these molecules. Herein, instead of using the direction of the bond, the flow of electron density between pairs of atoms is considered. For TB, PB and CB, the flow of electron density is from the O of water to the C or N or S atoms of CO_2, N_2O and SO_2, respectively. For X–H···Y HB, it is opposite the direction of the bond. In a cyclic structure resulting from the interconnected network of NCBs, a reference NCB may experience different types of cooperativity depending on the flow of electron density around it. For instance, consider the situations of an O···C TB between water and CO_2 molecule within the cyclic trimer and tetramer (*cf.* Scheme 1) involving CO_2 and 2 or 3 water molecules. The respective water molecules are labelled with their O atoms as O1, O2, and O3. In Scheme 1, the flow of electron density is shown in blue arrows. Depending upon the directions of these arrows (flow of electron density), a referenced TB experiences different types of cyclic cooperativity.

For example, in a cyclic trimer (*cf.* Scheme 1(a)), the direction of the flow of electron density between the three NCBs is the same (unidirectional). Therefore, the referenced TB between the C-atom CO_2 and O2 of water experiences a nice flow of electron density (as also shown by the full blue dotted circle) around this TB. In other words, the referenced TB experiences a full cyclic cooperativity (FCC). A similar FCC is also revealed by a TB in a cyclic tetramer, as shown in Scheme 1(c). These TBs are observed to have a positive cooperativity owing to the formation of an interconnection of a network of NCBs with adjacent molecules. However, in the cyclic trimer shown in Scheme 1(b), the directions of the flow of electron density between C1···O2 TB and O2···O1 HB are opposite. A similar situation of flow of electron density is found in cyclic tetramers shown in Scheme 1(e). Note that in these structures, the flow of electron density is broken between the adjacent TB and HB. Therefore, the referenced TB (between C1 and O2) in these structures experiences anti-cooperativity (AC). The reference TB in these cyclic structures would have a negative cooperativity contribution. The intermediate situation is shown in

15962 | *Phys. Chem. Chem. Phys.*, 2025, **27**, 15960–15974

This journal is © the Owner Societies 2025

Scheme 1 Representation of a TB in cyclic trimers exhibiting full cyclic cooperativity (a) or anticooperativity (b) and in cyclic tetramers exhibiting full cooperativity (c), partial cooperativity (d) and anticooperativity (e). See the text for details.

Scheme 1(d). The directions of flow of electron density between O1···O2, O2···C1, and O4···O5 are all the same (unidirectional). However, this unidirectionality is broken at the HB between O1 and O5 (*cf.* Scheme 1(d)). In other words, the unidirectionality of the referenced TB between O2 and C1 is partially conserved. The TB in this cyclic tetramer (Scheme 1(d)) is said to experience positive partial cyclic cooperativity (PCC). Similarly, different types (FCC, PCC or AC) of cyclic cooperativity may be experienced by the pnictogen and chalcogen bonds between the O atom of a water molecule (electron donor) and the N- or S-atom (electron acceptor) of N_2O or SO_2. These situations of cyclic cooperativity corresponding to PB and CB are shown in Schemes S1 and S2 in the ESI.† The discussion of these is skipped herein for brevity.

Synergetic energies of tetrel bonds in microhydrated clusters of carbon dioxide

The MP2/6-311++G(d,p) optimized geometries of $CO_2(H_2O)_n$, n = 3–5 clusters, are displayed in Fig. 2. Herein, the molecular clusters are labelled according to the number of water molecules and the cluster stability. For instance, in the label CWnA or CWnB, 'C' and 'W', respectively, represent carbon dioxide and water molecules, and 'n' is the number of water molecules in the given cluster. Label A corresponds to the energetically most stable cluster; the next one is denoted by label B and so on. Note that only geometries in which at least one TB bond is found to be common to two or more cyclic structures formed by the interconnected networks of NCBs are considered. To discuss the synergetic effect of the cyclic cooperativity, other geometries are not useful; hence, our discussion is restricted to the $CO_2(H_2O)_n$, n = 3–5 clusters, as shown in Fig. 2. As depicted in Fig. 2, in large 3D molecular clusters, a TB common to two or more cyclic structures (labelled as 'a', 'b', 'c', and 'd' cycles) may experience FCC, PCC, or AC. Consider the geometry of the **CW3B** cluster (*cf.* Fig. 2 and Scheme S3 in ESI†). In this geometry, a C···O **TB1** between CO_2 and water molecule is common to two trimeric **cycles a** and **b** (Scheme S3 in ESI†). Both of these cyclic trimers exhibit the full cyclic cooperativity (FCC) towards **TB1** common to them. It is postulated here that the strength of **TB1** is determined solely by the total CCs of the two cyclic trimers common to **TB1**. In other words, the numerical addition of the CC of these cyclic trimers when added to

the energy of **TB1** in the respective isolated CO_2···H_2O dimer (chopped out of CW3B cluster) gives the energy of **TB1** in the CW3B cluster. To establish this, the CC towards **TB1** from these two cycles is calculated using the MTA-based method.[45]

Scheme 2 illustrates the fragmentation procedure of the MTA-based method for the estimation of energy and CCs towards **TB1** in **cyclic trimer a**, consisting of CO_2, and two water molecules denoted by O2 and O3. Recall that the **TB1** corresponds to the C1···O2 interaction between CO_2 and the water molecule O2. Hence, **cyclic trimer a** is divided into two primary fragments: F1 (obtained by removing water O2) and F2 (obtained by removing the CO_2 molecule).

Putting fragments F1 and F2 together, one may regenerate the geometry of this **cyclic trimer a**. However, such regenerated geometry reveals two features: (i) the **TB1** between C1 and O2 present in **cyclic trimer a** is missed out, and (ii) there is a double counting of the common structural part (*viz.* water molecule O3) between F1 and F2 (*cf.* Scheme 2). This water molecule O3 is denoted as fragment F3. Upon the addition of SP energies of fragments F1 and F2 and subtraction of the energy of fragment F3, the energy of **cyclic trimer a** may be obtained. However, this energy of **cyclic trimer a** misses out on the **TB1** energy (E_{TB1}). Therefore, the **TB1** energy in this **cyclic trimer a** is calculated as $E_{TB1}^{\text{cyclic trimer a}} = (E_{F1} + E_{F2} - E_{F3}) - E_{\text{cyclic trimer a}} = 3.28$ kcal mol^{-1} at the MP2/aug-cc-pVTZ level. For E_{F1}, E_{F2}, E_{F3}, and $E_{\text{cyclic trimer a}}$, see Table S1 in ESI.† Note that $E_{TB1}^{\text{cyclic trimer a}}$ includes the CC coming from the interconnected network of HBs with **TB1** formed by an additional water O3 molecule in this **cyclic trimer a**. Therefore, this $E_{TB1}^{\text{cyclic trimer a}}$ value is different from the **TB1** energy in the respective isolated CO_2···water O2 dimer (E_{TB1}^{dimer}). The latter is obtained by applying a supermolecular approach as follows: $E_{TB1}^{\text{dimer}} = E_{C1\cdots O2}^{\text{dimer}} - \left(E_{CO_2}^{\text{monomer}} + E_{\text{water O2}}^{\text{monomer}}\right) = 2.72$ kcal mol^{-1}. For $E_{C1\cdots O2}^{\text{dimer}}$, $E_{CO_2}^{\text{monomer}}$, and $E_{\text{water O2}}^{\text{dimer}}$, see Table S1 in ESI.† This E_{TB1}^{dimer} value does not have a CC. The difference between $E_{TB1}^{\text{cyclic trimer a}}$ and E_{TB1}^{dimer} gives CC to the **TB1** in this **cyclic trimer a**, *i.e.* $E_{\text{cyclic trimer a}}^{\text{coop.}} = 0.56$ kcal mol^{-1}. Note that in this **cyclic trimer a**, the directions of electron density flow for all the three bonds (one TB and two HBs) are the same (unidirectional), which agrees with the calculated positive value of CC.
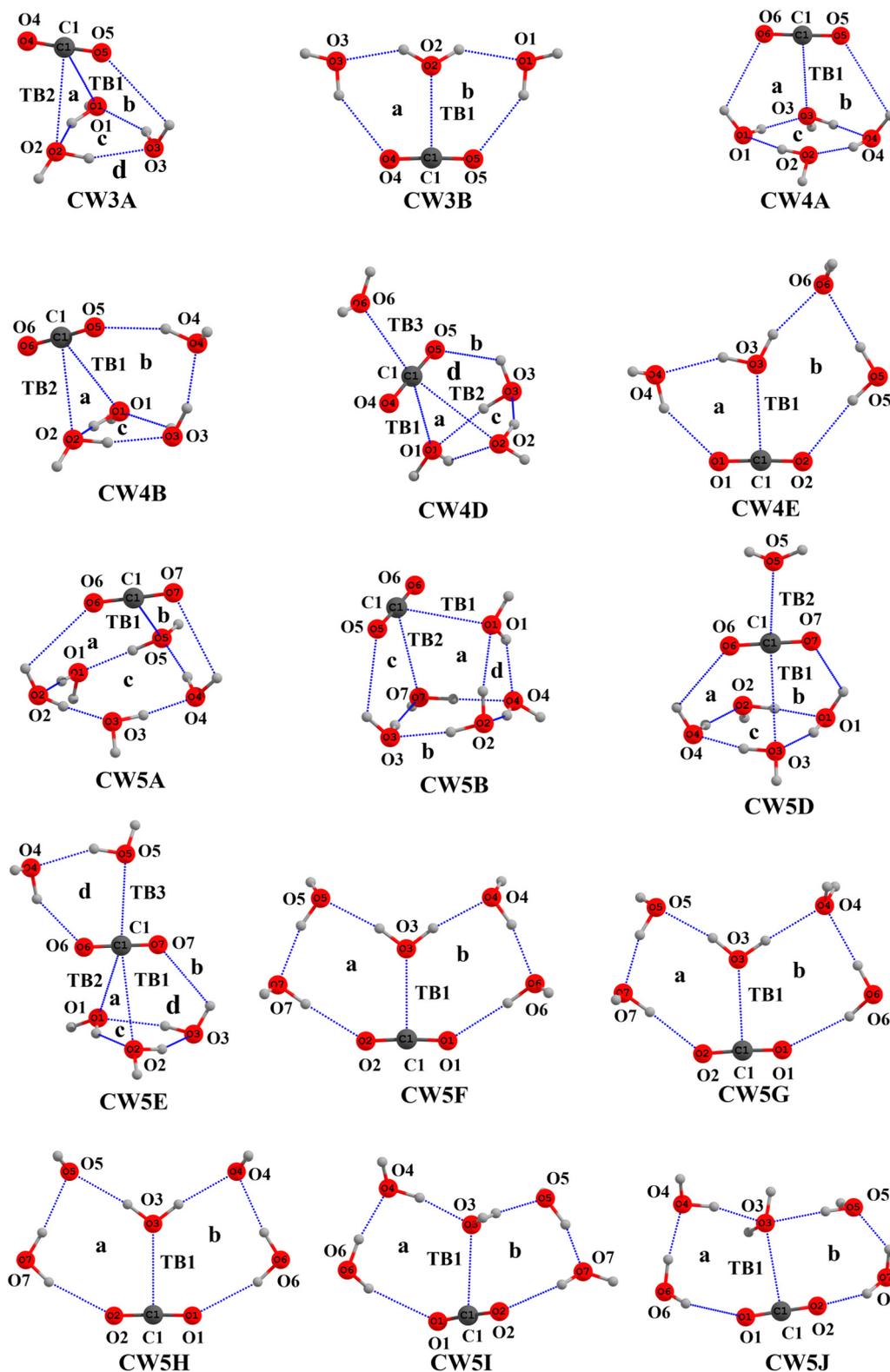
This journal is © the Owner Societies 2025

Phys. Chem. Chem. Phys., 2025, **27**, 15960–15974 | **15963**

Fig. 2 MP2/6-311++G(d,p) optimized geometries of $CO_2(H_2O)_n$, n = 3–5 clusters.

Similarly, the energy of **TB1** and the CC in the **cyclic trimer b** (*cf.* Fig. 2) is calculated using the MTA-based method to be $E_{\text{TB1}}^{\text{cyclic trimer b}}$ = 3.29 and $E_{\text{cyclic trimer b}}^{\text{coop.}}$ = 0.57 kcal mol^{-1},

respectively (*cf.* Schemes S3 and S4 in ESI†). Recall that this **cyclic trimer b** also exhibits FCC, which agrees with the calculated positive value of CC. Therefore, the total CC of **cyclic**
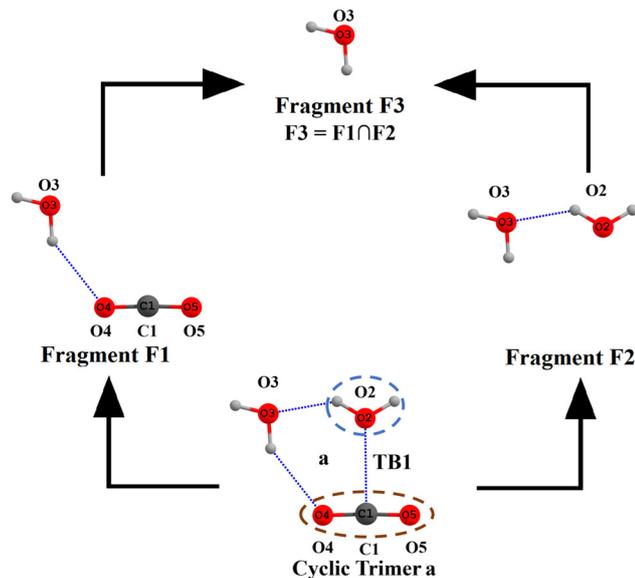
Scheme 2 Fragmentation procedure of the MTA-based method for calculating the energy of **TB1** in the **cyclic trimer a** of the CW3B cluster.

Table 1 TB energies (in kcal mol^{-1}) in $CO_2(H_2O)_n$, n = 3 to 5 cluster, along with the TB energy in the respective dimer species (E_{TB}^{dimer}). All calculations were performed at the MP2/aug-cc-pVTZ level of theory. See Fig. 2 and the text for details

TB	E_{TB}^{Dimer}	$E_{coop.}^{Cycle1}$	$E_{coop.}^{Cycle2}$	$E_{TB}^{Synergetic}$	$E_{TB}^{Actual\ Cluster}$	$|\Delta E_{TB}|$
CW3A						
TB1	1.21	−0.21	−0.10	0.90	0.84	0.06
TB2	2.42	0.40	−0.10	2.72	2.66	0.06
CW3B						
TB1	2.72	0.56	0.57	3.85	3.78	0.07
CW4A						
TB1	2.09	−0.24	0.43	2.28	2.08	0.20
CW4B						
TB1	1.12	−0.23	−0.13	0.76	0.69	0.07
TB2	2.44	−0.13	0.81	3.11	3.05	0.05
CW4D						
TB1	1.24	−0.05	−0.23	0.96	0.88	0.08
TB2	2.16	−0.05	0.41	2.52	2.34	0.18
CW4E						
TB1	2.90	0.85	0.21	3.96	3.90	0.06
CW5A						
TB1	2.43	0.64	−0.21	2.86	2.52	0.34
CW5B						
TB1	1.93	−0.01	−0.01	1.90	1.91	0.01
TB2	1.88	−0.01	−0.26	1.61	1.67	0.07
CW5D						
TB1	1.83	0.40	−0.25	1.98	1.68	0.30
CW5E						
TB1	1.21	−0.08	−0.20	0.94	1.01	0.07
TB2	2.21	−0.08	0.40	2.53	2.31	0.22
CW5F						
TB1	2.94	1.02	1.02	4.98	4.90	0.08
CW5G						
TB1	2.88	0.85	0.45	4.18	4.14	0.04
CW5H						
TB1	2.93	0.44	0.44	3.80	3.78	0.02
CW5I[a]						
TB1	1.85	−0.41	0.88	2.32	2.35	0.03
CW5J[a]						
TB1	0.49	−0.56	−0.15	−0.21	−0.18	0.03

[a] Partially optimized.

trimers **a** and **b** towards **TB1** is $E_{TB1}^{Total\ ccop.} = 0.56 + 0.57 = 1.13$ kcal mol^{-1}. This total CC when added to the **TB1** energy in the isolated dimer gives the synergetic energy of **TB1** in the **CW3B** cluster, *i.e.* $E_{TB1}^{Synergetic} = E_{TB1}^{dimer} + E_{TB1}^{Total\ coop.} = 2.72 + 1.13 = 3.85$ kcal mol^{-1}. The **TB1** energy in the actual **CW3B** cluster by applying the MTA-based method is also evaluated; see Scheme S5 in ESI† and discussion below it. The **TB1** energy obtained by applying the MTA-based method employing the actual CW3B cluster ($E_{TB1}^{CW3B} = 3.78$ kcal mol^{-1}) instead of cyclic trimers is very similar to the $E_{TB1}^{Synergetic}$ value. The absolute difference ($|\Delta E_{TB}|$) is small (0.07 kcal mol^{-1}). This small $|\Delta E_{TB}|$ value suggests that the **TB1** strength in the **CW3B** cluster is accurately calculated using the proposed method of synergetic cyclic cooperativity.

With this understanding, the energies of tetrel bonds in various geometries of $CO_2(H_2O)_n$, n = 3 to 5 clusters (*cf.* Fig. 2) by the present synergetic cyclic cooperativity approach and also by the MTA-based method employing actual clusters are evaluated. These TB energies in $CO_2(H_2O)_n$, n = 3 to 5 clusters, calculated by applying these two methods are compared in Table 1.

As shown in Table 1 and Fig. 2, two TBs (**TB1** and TB2) are present in the **CW3A** cluster. The **TB1** bond is common to two trimeric **cycles a** (consisting of O1, O2 and CO$_2$) and **b** (consisting of O1, O3 and CO$_2$), both exhibiting AC as also reflected from their negative CCs (−0.21 and −0.1 kcal mol^{-1}, respectively). The TB2 is also common to two trimeric cycles, *i.e.* **cycle a** (consisting of O1, O2 and CO$_2$) and **cycle d** (consisting of O2, O3 and CO$_2$). As discussed, trimeric **cycle a** exhibits AC. However, **cycle d** presents an FCC in which the flow of electron density between bonds is unidirectional. This FCC nature of **cycle d** is also evident from the positive value of CC (0.40 kcal mol^{-1}). Therefore, the calculated energy of TB2 is (2.72 kcal mol^{-1}) larger

than that of **TB1** (0.90 kcal mol^{-1}). Importantly, these calculated values of **TB1** and **TB2** by applying the method of synergetic cyclic cooperativity are in excellent agreement with their actual cluster counterparts (0.84 and 2.66 kcal mol^{-1}) calculated using the MTA-based method.

In the **CW4A** cluster, **TB1** is common to two trimeric **cycles a** and **b**. Here, **cycle a** bears AC; the direction of the flow of electron density between O3···O1 and O3···C1 is opposite to each other. This AC nature of **cycle a** is also evident in the negative value of CC (−0.24 kcal mol^{-1}) to **TB1**. However, trimeric **cycle b** exhibits FCC (*cf.* Fig. 2) with positive CC (0.43 kcal mol^{-1}) to **TB1**. By adding the total CC of both of these cycles to **TB1** energy in the isolated dimers, the synergetic **TB1** energy is obtained to be 2.28 kcal mol^{-1}. This **TB1** energy is in good agreement with its energy (2.08 kcal mol^{-1}) in the actual **CW4A** cluster calculated by applying the MTA-based method. The structure of **CW4B** is very similar to that of CW3A, except that there is an extra water molecule, O4, between O3 and the CO$_2$ molecule. The **TB1** of **CW4B** is common to one trimeric AC (CC = −0.13 kcal mol^{-1}) **cycle a** (consisting of two water molecules O1, O2 and CO$_2$ molecule) and one tetrameric **cycle**

This journal is © the Owner Societies 2025

Phys. Chem. Chem. Phys., 2025, **27**, 15960–15974 | **15965**

b (consisting of three water molecules O1, O3, O4 and CO_2 molecule), which also exhibits AC (CC = -0.23 kcal mol^{-1}) (Scheme S6 in ESI†). The **TB2** of **CW4B** is common to one trimeric AC (CC = -0.13 kcal mol^{-1}) **cycle a** and one tetrameric **cycle d** (consisting of three water molecules O2, O3, and O4 and a CO_2 molecule), which exhibits FCC (CC = 0.81 kcal mol^{-1}). Because of this FCC nature of **cycle d**, the **TB2** (3.11 kcal mol^{-1}) is stronger than **TB1** (0.76 kcal mol^{-1}). In the optimized structure of **CW4C**, there is only one tetrameric cycle, which consists of **TB1**. Therefore, its geometry for the discussion of its energy evaluation by the synergetic cooperativity evaluation is not considered. The next important cluster is the **CW4D** cluster, consisting of three tetrel bonds, *viz.* **TB1**, **TB2** and **TB3**. Of these TBs, **TB3** is not a part of any cyclic structure; therefore, its discussion is skipped herein, and its energy can be evaluated using the direct MTA-based method. The **TB1** is common to two trimeric **cycles**, **a** (consisting of water molecules O1, O2, and CO_2) and **b** (consisting of two water molecules O1, O3, and CO_2), both bearing AC with CCs of -0.05 and -0.23 kcal mol^{-1}, respectively. The **TB2** is also common to AC trimeric **cycle a** and **cycle d** (consisting of water molecules O2, O3, and CO_2), which bears an FCC (CC = 0.41 kcal mol^{-1}). Therefore, the synergetic energy of **TB2** (2.52 kcal mol^{-1}) is larger than that of **TB1** (0.96 kcal mol^{-1}). The **CW4E** is an interesting cluster. Here, the tetrel bond **TB1** is common to one trimeric **cycle a** (consisting of O3 and O4 water molecules and CO_2) bearing FCC and another tetrameric **cycle b** (consisting of O3, O5, and O6 water molecules and CO_2), which exhibits partial cyclic cooperativity (PCC). Because of these positive FCC (0.85 kcal mol^{-1}) and PCC (0.21 kcal mol^{-1}) contributions of these cyclic structures, synergistic **TB1** energy (3.96 kcal mol^{-1}) is the largest among all CW4 clusters. This energy calculated by the synergistic effect of cyclic cooperativity is in good agreement with its actual cluster counterpart (3.90 kcal mol^{-1}) calculated by applying the MTA-based method.

In the **CW5A** cluster (*cf.* Fig. 2), **TB1** is common to AC trimeric **cycle b** and FCC tetrameric **cycle a**, with CC contributions of -0.21 and 0.64 kcal mol^{-1}, respectively. The calculated synergetic energy of **TB1** is 2.86 kcal mol^{-1}, which is in good agreement with the one calculated by applying the MTA-based method with the actual **CW5A** cluster (2.52 kcal mol^{-1}). In the **CW5B** cluster, **TB1** is common to two tetrameric **cycles a** (consisting of O1, O4, and O7 water molecules and CO_2) and **b** (consisting of O1, O2, and O3 water molecules and CO_2), both bearing AC (CC = -0.01 kcal mol^{-1} for both cycles); see Scheme S6 in ESI.† Because of these two AC cycles, the energy of **TB1** is very small, 1.9 kcal mol^{-1}. The energy of **TB2** in this **CW5B** cluster is even smaller (1.61 kcal mol^{-1}), which may be attributed to the fact that **TB2** is common to one tetrameric **cycle a** and trimeric **cycle c** (consisting of O3 and O7 water molecules and CO_2), both bearing AC (*cf.* Scheme S6 in ESI†) with CC values of -0.01 and -0.24 kcal mol^{-1}, respectively. These synergistic energies of **TB1** and **TB2** are in excellent agreement with their actual cluster counterparts (*cf.* Table 1). In the **CW5D** cluster, **TB1** is common to two trimeric cycles: **a** (consisting of O3 and O4 water molecules and CO_2) and **b** (consisting of O3,

O1 water molecules and CO_2). Former **cycle a** bears FCC with a CC of 0.40 kcal mol^{-1}. However, trimeric **cycle b** exhibits AC with a CC of -0.25 kcal mol^{-1}. The calculated synergetic energy of **TB1** is 1.98 kcal mol^{-1} is in good agreement with the one calculated by applying the MTA-based method employing the actual **CW5D** cluster (1.68 kcal mol^{-1}). The structure of the **CW5E** cluster is similar to that of the **CW4D** cluster, except that the additional water molecule forms a cyclic structure involving **TB3**. The calculated synergistic energies of **TB1** (0.94 kcal mol^{-1}) and **TB2** (2.53 kcal mol^{-1}) in the **CW5E** cluster are similar to those in the **CW4D** (0.96 and 2.52 kcal mol^{-1}) cluster. The energies of **TB1** in **CW5F**, **CW5G**, **CW5H**, **CW5I**, and **CW5J** clusters, wherein **TB1** is common to two tetrameric cycles, are discussed. Although these structures of clusters look similar, they differ in terms of cooperativity exhibited by the two tetrameric cycles towards **TB1**. For instance, two tetrameric **cycles** (**a** and **b**) exhibit FCC in the **CW5F** cluster (*cf.* Fig. 2), as is evident from positive CCs (1.02 kcal mol^{-1}) for both the cycles (*cf.* Table 1). Because of these positive CCs of both cycles, the **TB1** energy (4.98 kcal mol^{-1}) is largest among all the CW$_n$ (n = 3–5) clusters studied herein. The energy of **TB1** is slightly smaller (4.18 kcal mol^{-1}) in the **CW5G** cluster compared to the **CW5F** cluster. This may be because in the **CW5G** cluster, tetrameric **cycle a** exhibits FCC (CC = 0.85 kcal mol^{-1}) to **TB1**, while **cycle b** bears partial cyclic cooperativity (PCC) with smaller but positive CC (0.45 kcal mol^{-1}). However, since both the **cycles** (**a** and **b**) in the **CW5H** cluster (*cf.* Fig. 2) exhibit PCC with CC of each being 0.44 kcal mol^{-1}. The energy of **TB1** is smaller (3.80 kcal mol^{-1}) than its value in **CW5F** and **CW5G** clusters. A partially optimized **CW5I** cluster is also considered, wherein **TB1** is at the interface of two cyclic tetrameric structures, of which one exhibits AC (**cycle a**) and the other shows FCC (**cycle b**) (Fig. 2). The CC of **cycle a** is -0.41 kcal mol^{-1} and that of **cycle b** is 0.88 kcal mol^{-1}, which is consistent with the nature of these cyclic structures. Another partially optimized cluster is **CW5J**, wherein **TB1** is at the interface of two tetrameric **cycles a** and **b**, both exhibiting AC. The CC of **cycle a** is -0.56 kcal mol^{-1} and that of **cycle b** is -0.15 kcal mol^{-1}, which are consistent with their AC nature. Although the **TB1** energy in the isolated dimer is small and positive, the energy of **TB1** in the actual cluster is small and negative (-0.21 kcal mol^{-1}). The energy of **TB1** calculated by the synergistic cooperative effects of the two cycles is in excellent agreement with its value calculated by full calculation using the MTA-based method (-0.18 kcal mol^{-1}). The negative value indicates that this bond is unstable in the cluster compared to when it is isolated as a dimer. Note that the structures exhibiting one or two AC cycles are partially optimized (with frozen atoms). These structures cannot be fully optimized in the present form. The reason could be the instability of these structures because of the formation of AC cycle(s). It is emphasized here that the interplay of the nature of cyclic structures common to a TB in all the CW$_n$ (n = 3–5) clusters studied in this work is nicely reflected in the calculated synergistic energy of such TBs. This suggests the robustness of the proposed methodology. Importantly, all the calculated synergistic energies of TBs in various CW$_n$ (n = 3–5) clusters are in excellent

15966 | *Phys. Chem. Chem. Phys.*, 2025, **27**, 15960–15974

This journal is © the Owner Societies 2025

agreement with their full-calculation counterparts. The maximum absolute difference between two values ($|\Delta E_{TB}|$) is less than 0.4 kcal mol^{-1}, suggesting that the present approach of synergistic cooperativity provides accurate estimates of the energy of various tetrel bonds in $CO_2(H_2O)_n$ clusters.

Synergetic energies of pnictogen bonds in microhydrated clusters of nitrous oxide

Similarly, various pnictogen bonds (PB), which are at the interface of two or more cyclic structures formed owing to interconnected networks of NCBs in microhydrated clusters of nitrous oxide (N_2O), are investigated. The MP2/6-311++G(d,p) optimized geometries of various microhydrated clusters N_2O, *viz.* the $N_2O(H_2O)_n$, n = 3–5 clusters, are shown in Fig. 3.

Herein, these clusters are labelled similar to $CO_2(H_2O)_n$ clusters, *i.e.* according to the number of water molecules and the cluster stability. For instance, in the label NWnA or NWnB, 'N' and W represent nitrous oxide and water molecule, respectively. 'n' is the number of water molecules in a given cluster. Label A corresponds to the energetically most stable cluster; the next one is denoted by label B and so on. Further, only geometries wherein at least one PB bond is found to be common to two or more cyclic structures are considered (Fig. 3). As depicted in Fig. 3, similar to a TB, a PB is found to be common to two or more cyclic structures and may experience an FCC, PCC, or AC in these microhydrated N_2O clusters. For instance, consider the geometry of the **NW3C** cluster shown in Fig. 3. In this geometry, an N···O pnictogen bond (**PB1**) between N_2O and a water molecule is common to two **cyclic trimers a** and **b**. Both of these cyclic trimers exhibit the FCC to **PB1**. Therefore, the energy of this **PB1** can be determined by the total CCs of these two cyclic trimers. The CCs towards PB1 of both cycles are estimated by applying the MTA-based method. For details of fragmentation procedures for the calculation of **PB1** energy and the respective CCs in **cycles a** and **b**, see Schemes S7 and S8 in ESI.† The **PB1** energy along with the respective CCs of each of these trimeric cycles is reported in Table 2. As shown in Table 2, the cooperativity contributions of the two cycles are 0.41 and 0.30 kcal mol^{-1}, respectively. The calculated positive CCs are consistent with the FCC nature of these two cycles. When these two CCs are added to the energy of **PB1** in the respective dimer, the synergetic energy of **PB1** in the **NW3C** cluster is obtained to be 3.05 kcal mol^{-1}. This calculated energy of **PB1** is in excellent agreement with its value in the actual cluster counterparts (2.95 kcal mol^{-1}) calculated by applying the MTA-based method; see Scheme S9 in ESI† for the fragmentation procedure. The difference between the energy of **PB1** calculated by these two approaches is negligibly small (0.1 kcal mol^{-1}), indicating that the proposed method of synergetic cooperativity also provides an accurate estimation of the energy of PB. It is mentioned here that this is the only tri-hydrated N_2O cluster structure wherein the PB1 is found to be common to two trimeric cyclic structures. The other lower energy conformers, *viz.* **NW3A** and **NW3B** clusters, have PB1 as part of only one cycle (Scheme S10 in ESI†).

With this understanding of the method of the synergetic cyclic cooperativity predicting the accurate energy of PB1 in the **NW3C** cluster, this method is applied to determine the energy of various PBs in higher order (n = 4 and 5) microhydrated clusters of N_2O. For instance, in the **NW4A** cluster, the N_2O molecule seems to interact with the water tetramer, forming a **PB1** bond common to two trimeric **cycles a** and **b**. Herein, **cycle a** bears an AC, while **cycle b** bears an FCC. The AC and FCC natures of these cycles are nicely reflected in terms of the calculated CCs being −0.20 and 0.40 kcal mol^{-1}, respectively. By adding the total CCs of these cycles to **PB1** energy in the isolated dimers, the synergetic **PB1** energy is obtained (2.30 kcal mol^{-1}), which is in good agreement with its value (2.00 kcal mol^{-1}) in the actual **NW4A** cluster calculated by applying the MTA-based method. The structure of **NW4B** is somewhat different from that of **NW4A**. In **NW4B**, a cyclic water trimer (denoted as **d**) interacts with the N_2O molecule, forming two bifurcated pnictogen bonds: **PB1** and **PB2**. The fourth water molecule (denoted by O2) forms two HBs: one with the terminal N of N_2O and the other with the H of water O2 (*cf.* Fig. 3). The **PB1** is at the intersection of one trimeric **cycle b** (consisting of N_2O, O1 and O5 water molecules) and one tetrameric **cycle a** (consisting of N_2O, and three water molecules O1, O2, and O3), both exhibiting AC to **PB1** (Scheme S11 in ESI†). The AC nature of these two cyclic structures common to **PB1** is nicely reflected in their negative CCs to **PB1** (−0.10 and −0.24 kcal mol^{-1}, respectively). Thus, the calculated synergetic **PB1** energy is very small (0.91 kcal mol^{-1}). However, **PB2** is common to one trimeric AC **cycle b** (also common to **PB1**) and a tetrameric **cycle c** (consisting of N_2O, and three water molecules O3, O2 and O5) bearing FCC to **PB2** (*cf.* Scheme S11 in ESI†). The CC of FCC **cycle c** is 0.73 kcal mol^{-1}. This is the reason that the synergetic energy of **PB2** is larger (2.94 kcal mol^{-1}) than that of **PB1**. The energy of **PB1** and **PB2** calculated by the method of synergetic cyclic cooperativity is in excellent agreement with their actual cluster counterparts calculated by applying the MTA-based method (*cf.* Table 2). The difference in the energy calculated by applying the two methods is less than 0.08 kcal mol^{-1}. The structure of the **NW4D** cluster is similar to that of the **NW4B** cluster except that the **PB2** of **NW4B** is converted to HB between water and the terminal O-atom of N_2O. Therefore, there is only a **PB1** bond, which is at the interface of one trimeric **cycle a** bearing an FCC and the other tetrameric **cycle b** bearing an AC (*cf.* Fig. 3). The respective CCs of these two cycles are 0.22 and −0.12 kcal mol^{-1}. The synergetic energy of **PB1** is 2.22 kcal mol^{-1}, which is in excellent agreement with its actual cluster counterpart (2.16 kcal mol^{-1}). In **NW4E**, there are three pnictogen bonds (**PB1**, **PB2** and **PB3**). The energy of **PB1** and **PB2** can be obtained using the method of synergetic cyclic cooperativity. The **PB1** is at the intersection of two AC trimeric **cycles a** (consisting of N_2O and two water O1 and O3 molecules) and **b** (consisting of N_2O and two water molecules O1 and O2). The AC nature of these cycles is also reflected in the respective negative CCs (−0.08 and −0.21 kcal mol^{-1}), resulting in a weak ($E_{PB1}^{Synergetic}$ = 1.03 kcal mol^{-1} and E_{PB1}^{actual} = 1.00 kcal mol^{-1}) **PB1** bond. AC **cycle b** is also common to **PB2** along with FCC

This journal is © the Owner Societies 2025

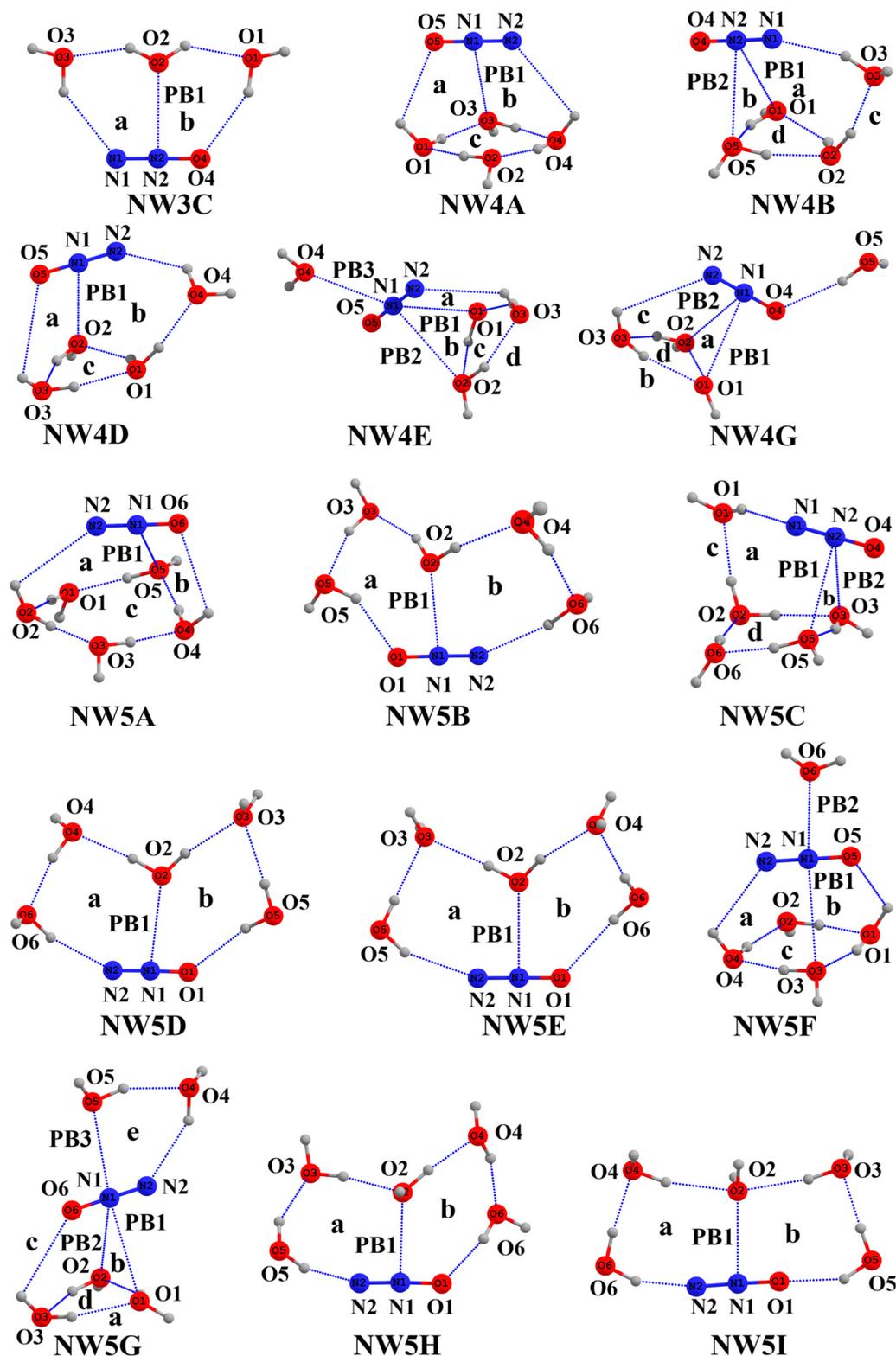*Phys. Chem. Chem. Phys.*, 2025, **27**, 15960–15974 | **15967**

Fig. 3   MP2/6-311++G(d,p) optimized geometries of $N_2O(H_2O)_n$, $n = 3–5$ clusters.

trimeric **cycle d** (consisting of N_2O and two water molecules O2 and O3). The positive CCs (0.37 kcal mol^{-1}) of FCC **cycle d** along with the small AC of **cycle b** (-0.06 kcal mol^{-1}) make **PB2** stronger ($E_{PB2}^{Synergetic}$ = 2.52 kcal mol^{-1} and E_{PB2}^{actual} = 2.32 kcal mol^{-1})

than **PB1**. The structure of **NW4G** is similar to that of **NW4E**, except that the fourth water molecule forms HB with the O-atom of N_2O instead of **PB3**. The smaller synergistic energy of **PB1** (1.12 kcal mol^{-1}) than that of **PB2** (2.48 kcal mol^{-1}) in

15968 | *Phys. Chem. Chem. Phys.*, 2025, **27**, 15960–15974

This journal is © the Owner Societies 2025

Table 2 PB energies (in kcal mol^{-1}) in N$_2$O(H$_2$O)$_n$, n = 3 to 5 cluster, along with the PB energy in the respective dimer species (E_{PB}^{dimer}). All calculations were performed at the MP2/aug-cc-pVTZ level of theory. See Fig. 3 and the text for details

PB	E_{PB}^{Dimer}	$E_{coop.}^{Cycle1}$	$E_{coop.}^{Cycle2}$	$E_{PB}^{Synergetic}$	E_{PB}^{actual}	$|\Delta E_{PB}|$
NW3C						
PB1	2.34	0.41	0.30	3.05	2.95	0.10
NW4A						
PB1	2.10	−0.20	0.40	2.30	2.00	0.30
NW4B						
PB1	1.25	−0.10	−0.24	0.91	0.83	0.08
PB2	2.31	−0.10	0.73	2.94	2.87	0.07
NW4D						
PB1	2.12	0.22	−0.12	2.22	2.16	0.06
NW4E						
PB1	1.32	−0.08	−0.21	1.03	1.00	0.03
PB2	2.21	−0.06	0.37	2.52	2.32	0.20
NW4G						
PB1	1.39	−0.10	−0.17	1.12	1.26	0.14
PB2	2.28	−0.10	0.30	2.48	2.40	0.08
NW5A						
PB1	2.33	0.51	−0.16	2.68	2.32	0.36
NW5B[a]						
PB1	2.02	0.17	0.77	2.96	2.86	0.10
NW5C						
PB1	2.51	−0.07	0.73	3.17	3.02	0.15
PB2	1.14	−0.08	−0.34	0.72	0.48	0.24
NW5D						
PB1	2.44	0.83	0.11	3.38	3.31	0.07
NW5E						
PB1	2.63	0.18	0.37	3.18	3.15	0.02
NW5F						
PB1	1.97	0.38	−0.23	2.12	1.77	0.35
NW5G						
PB1	1.34	−0.08	−0.15	1.11	1.21	0.10
PB2	2.29	−0.09	0.33	2.53	2.28	0.25
NW5H[a]						
PB1	1.39	−0.19	0.65	1.85	1.85	0.00
NW5I[a]						
PB1	1.03	−0.07	−0.17	0.79	0.88	0.09

[a] Partially optimized.

the **NW4G** cluster may be similarly explained. Importantly, these energies of **PB1** and **PB2** are in excellent agreement with those calculated by employing the actual **NW4G** cluster in the MTA-based method.

Similar to a tetra-hydrated **NW4A** cluster, the most stable **NW5A** cluster has a cyclic water pentamer interacting with N$_2$O, forming a **PB1** bond common to one tetrameric FCC **cycle a** and one trimeric AC **cycle b**. The FCC and AC natures of these cyclic structures are nicely reflected in the calculated positive (0.51 kcal mol^{-1}) and negative (−0.16) CCs. Upon adding these CCs to the **PB1** energy in the isolated ON$_2$···water dimer, synergetic **PB1** energy (2.68 kcal mol^{-1}) is obtained. This synergetic **PB1** energy is in good agreement with its value (2.32 kcal mol^{-1}) obtained using the MTA-based method with the actual **NW5A** cluster. In the higher energy penta-hydrated clusters, the N$_2$O molecule interacts with cyclic water tetramer (**NW5C** and **NW5F**) and cyclic water trimer (**NW5G**). In the **NW5C** cluster, there are two PBs (**PB1** and **PB2**). The **PB1** is common to one AC trimeric **cycle b** (consisting of N$_2$O and water molecules O3 and O5) and an FCC pentameric **cycle a** (consisting of N$_2$O and O1, O2, O6, and O5 water molecules;

see Scheme S11 in ESI.† The AC and FCC natures of these cycles result in negative (−0.07 kcal mol^{-1}) and positive (0.73 kcal mol^{-1}) CCs to **PB1**, respectively. The synergetic energy of **PB1** is 3.17 kcal mol^{-1}, which is in good agreement with its value (3.02 kcal mol^{-1}) in the actual **NW5C** cluster. However, the energy of **PB2** is much smaller (0.72 kcal mol^{-1}) compared to that of **PB1**. This may be attributed to the fact that **PB2** resides at the interface of two AC cycles, *viz.* trimeric **cycle b** (also common to **PB1**) and tetrameric **cycle c** (consisting of N$_2$O and O1, O2, and O3 water molecules). The negative CCs (−0.08 and −0.34 kcal mol^{-1}) of these cycles make **PB2** very weak. In the **NW5F** cluster, **PB1** is at the intersection of one FCC (**cycle a**) and another AC (**cycle b**) trimeric cycle with their respective CCs being 0.38 and −0.23 kcal mol^{-1}, respectively. The synergetic energy of **PB1** is 2.12 kcal mol^{-1}, and that in the actual **NW5F** cluster is very close to it (1.77 kcal mol^{-1}). The structure of **NW5G** is similar to that of **NW4G** discussed above, except that the 5th water molecule (denoted as O5) forms HB with the 4th water molecule (O4) along with an additional PB (**PB3**). This **PB3** is part of only one cyclic structure; therefore, its energy can be evaluated using the standard MTA-based method employing the **NW5G** cluster. The **PB1** is at the intersection of two AC trimeric **cycles a** and **b** (*cf.* Scheme S11 in ESI†), with their respective CCs being −0.08 and −0.15 kcal mol^{-1}. Because of these two negative CCs, the energy of **PB1** is small ($E_{PB1}^{Synergetic}$ = 1.11 kcal mol^{-1} and E_{PB1}^{actual} = 1.21 kcal mol^{-1}, respectively). However, the **PB2** is common to one AC trimeric **cycle a** (also common to PB1) and another trimeric FCC **cycle c** (consisting of N$_2$O and O2 and O3 water molecules). The positive CC (0.33 kcal mol^{-1}) of this FCC **cycle c** and the small negative CC (−0.09 kcal mol^{-1}) of **cycle a** make **PB2** ($E_{PB2}^{Synergetic}$ = 2.53 kcal mol^{-1} and E_{PB2}^{actual} = 2.28 kcal mol^{-1}) stronger than **PB1**.

The structure of **NW5D** is interesting as it bears the **PB1** at the intersection of one FCC tetrameric **cycle a** (consisting of N$_2$O and O2, O4, and O6 water molecules) and another PCC tetrameric **cycle b** (consisting of N$_2$O and O2, O3, and O5 water molecules) (Fig. 3). The CCs of these cycles are 0.83 and 0.11 kcal mol^{-1}, respectively, leading to one of the strongest **PB1** bond ($E_{PB1}^{Synergetic}$ = 3.38 kcal mol^{-1} and E_{PB1}^{actual} = 3.31 kcal mol^{-1}, respectively). Starting from **NW5D**, various structures with a **PB1** bond at the intersection of two cycles (similar to **NW5D**) bearing different combinations of types of cooperativities are generated. For instance, in **NW5E**, both tetrameric cycles exhibit PCC to **PB1** with their respective CCs being 0.18 and 0.37 kcal mol^{-1}, making **PB1** slightly weaker ($E_{PB1}^{Synergetic}$ = 3.18 kcal mol^{-1} and E_{PB1}^{actual} = 3.15 kcal mol^{-1}) in **NW5E** compared to **PB1** in **NW5D**. In **NW5H**, tetrameric **cycle a** is AC (CC = −0.19 kcal mol^{-1}), while tetrameric **cycle b** is FCC (CC = 0.65 kcal mol^{-1}) with synergetic energy of **PB1** to be 1.85 kcal mol^{-1}, which is in good agreement with its value in the actual cluster (E_{PB1}^{actual} = 1.85 kcal mol^{-1}). It should be noted here that the **NW5H** structure is partially optimized. On full optimization, this combination of cyclic structures is not retained. Similarly, a partially optimized structure with both (**cycles a** and **b**) AC cycles (CCs: −0.07 and −0.17 kcal mol^{-1}, respectively) leads to the weakest **PB1** bond ($E_{PB1}^{Synergetic}$ = 0.79 kcal mol^{-1}

This journal is © the Owner Societies 2025

Phys. Chem. Chem. Phys., 2025, **27**, 15960–15974 | **15969**

and E_{PB1}^{actual} = 0.88 kcal mol^{-1}) among all the clusters in this class. It is emphasized here that the interplay of the nature of cyclic structures common to PBs in all **NWn** (n = 3–5) clusters is nicely reflected in their calculated synergistic energies, once again highlighting the robustness of the proposed approach. Importantly, all the calculated synergistic PB energies are in excellent agreement with their full-calculation counterpart with $|\Delta E_{PB}|$ falling between 0.00 and 0.36 kcal mol^{-1}.

Synergetic energies of chalcogen bonds in microhydrated clusters of sulphur dioxide

With the above understanding of the method of synergetic cyclic cooperativity for evaluating the accurate energy of TBs and PBs, the applicability of this method is tested for estimating the energy of chalcogen bonds (CBs) in microhydrated clusters of SO$_2$. Recall that the electron-deficient region around the S-atom of SO$_2$ interacts with the electron-rich O-atom of water to form a dimeric complex stabilized by a CB. The MP2/6-311++G(d,p) optimized geometries of various microhydrated clusters of SO$_2$, *viz.* SO$_2$(H$_2$O)$_n$, n = 3–5, are shown in Fig. 4. The nomenclature **SWn** of SO$_2$(H$_2$O)$_n$ clusters is similar to those of CO$_2$(H$_2$O)$_n$ and N$_2$O(H$_2$O)$_n$ clusters. As depicted in Fig. 4, a CB is also found to be common to two or more cyclic structures formed owing to the interconnected networks of HBs (HO–H$\cdots$O(H$_2$) and HO–H$\cdots$O(SO)) and a CB ((H$_2$)O$\cdots$SO$_2$). For instance, in the **SW3B** cluster, the **CB1** bond is common to two trimeric cycles: **a** and **b**. Therefore, the energy of this **CB1** can be calculated by adding the CCs of these cycles to its energy in the respective isolated dimer chopped out of the **SW3B** cluster. The CCs of these cycles were evaluated by applying the MTA-based method (Schemes S12–S14 in ESI†). The discussion of these schemes is very similar to those in Scheme 1 and Schemes S4, S5 (ESI†) for TB and Schemes S7–S9 (ESI†) for PB; therefore, we skipped it for brevity. As shown in Schemes S12 and S13 in ESI,† the CCs of these two trimeric cycles are 2.70 and 2.69 kcal mol^{-1}, which are consistent with the fact that both of these cycles exhibit positive FCC to **CB1** in the **SW3B** cluster. On adding the total CCs to the energy of **CB1** in the isolated H$_2$O$\cdots$SO$_2$ dimer (3.45 kcal mol^{-1}), the synergetic energy of **CB1** is obtained (8.84 kcal mol^{-1}), which is in good agreement with its value in the actual **SW3B** cluster (8.91 kcal mol^{-1}; see Scheme S14, ESI†), indicating that the proposed method also works for the CB.

With this understanding of the accurate evaluation of CB energy in the **SW3B** cluster, the synergetic cyclic cooperativity method is applied to different CBs in microhydrated **SWn** clusters. For example, in the lowest energy **SW3A** cluster, two bifurcated CBs are formed. The **CB1** is common to two trimeric cycles **a** and **b**, of which **cycle a** exhibits FCC (CC = 1.28 kcal mol^{-1}) while **cycle b** exhibits AC (CC = −0.38 kcal mol^{-1}); see Scheme S15 in ESI.† **Cycle b** is also common to **CB2** with the same value of CC. The other **cycle c** exerts AC to **CB2** (CC = −0.42 kcal mol^{-1}). Therefore, **CB2** is much weaker ($E_{CB2}^{Synergetic}$ = −0.16 kcal mol^{-1} and E_{CB2}^{actual} = −0.27 kcal mol^{-1}) than **CB1** ($E_{CB1}^{Synergetic}$ = 5.01 kcal mol^{-1} and E_{CB1}^{actual} = 4.90 kcal mol^{-1}) in the **SW3A** cluster. The negative **CB2** energy indicates the destabilization of this interaction in

the **SW3A** cluster compared to the isolated dimer (E_{CB2}^{Dimer} = 0.65 kcal mol^{-1}).

In the lowest energy **SW4A** cluster, the **CB1** bond is at the intersection of two trimeric cycles, of which one is AC (**cycle a**, CC = −0.76 kcal mol^{-1}) and the other is FCC (**cycle b**, CC = 1.80 kcal mol^{-1}). Because of these AC and FCC combinations of cyclic structures, the **CB1** in the **SW4A** cluster is of moderate strength ($E_{CB1}^{Synergetic}$ = 4.78 kcal mol^{-1} and E_{CB1}^{actual} = 4.43 kcal mol^{-1}). However, the **CB1** in the **SW4B** cluster is common to one FCC trimeric **cycle a** (CC = 1.75 kcal mol^{-1}) and another AC tetrameric **cycle b** (CC = 0.09 kcal mol^{-1}). Upon adding these CCs to **CB1** energy in the respective dimer, the obtained synergetic **CB1** energy (5.42 kcal mol^{-1}) is in excellent agreement with its value in the actual **SW4B** cluster (5.39 kcal mol^{-1}) calculated by applying the MTA-based method (Table 3). In the **SW4C** cluster, there are two CBs at the interface of the two cyclic structures. The **CB1** is common to trimeric **cycle b** (consisting of SO$_2$ and O1 and O4 water molecules) and tetrameric **cycle a** (consisting of SO$_2$ and O1, O2, and O3 water molecules), both exhibiting AC (Scheme S15 in ESI†). The respective negative CCs (−0.30 and −0.46 kcal mol^{-1}) make the **CB1** bond weak ($E_{CB1}^{Synergetic}$ = 0.12 kcal mol^{-1} and E_{CB1}^{actual} = −0.003 kcal mol^{-1}). However, **CB2** is at the intersection of trimeric **cycle b** (also common to **CB1**), exhibiting AC (CC = −0.46 kcal mol^{-1}) and tetrameric **cycle c** (consisting of SO$_2$ and O4, O2, and O3 water molecules), which shows FCC (CC = 1.82 kcal mol^{-1}). Because one of the cycles has a positive CC, the energy of **CB2** is moderate ($E_{CB1}^{Synergetic}$ = 4.90 kcal mol^{-1} and E_{CB1}^{actual} = 4.78 kcal mol^{-1}). In the **SW4D** cluster, the **CB1** bond is common to one PCC tetrameric **cycle a** (CC = 1.10 kcal mol^{-1}) and one FCC trimeric **cycle b** (CC = 2.38 kcal mol^{-1}). This makes **CB1** in the **SW4D** cluster one of the strongest ($E_{CB1}^{Synergetic}$ = 7.35 kcal mol^{-1} and E_{CB1}^{actual} = 7.37 kcal mol^{-1}) bond among all the tetra-hydrated complexes of SO$_2$.

In the lowest energy penta-hydrated **SW5A** cluster, the **CB1** bond is at the interface of two tetrameric cycles, of which one possesses FCC (**cycle a**) and the other possesses PCC (**cycle b**). The respective cooperativity contributions are 2.68 and 0.73 kcal mol^{-1}, making **CB1** one of the strongest bonds ($E_{CB1}^{Synergetic}$ = 7.32 kcal mol^{-1} and E_{CB1}^{actual} = 7.33 kcal mol^{-1}). In the **SW5B** cluster, the S atom is involved in the formation of two bifurcated CBs. Herein, **CB1** is common to two tetrameric **cycles a** (consisting of SO$_2$ and O1, O2, and O5 water molecules) and **b** (consisting of SO$_2$ and O1, O3, and O4 water molecules) (Scheme S15 in ESI†). **Cycle a** possesses an AC (CC = −0.86 kcal mol^{-1}), while **cycle b** possesses an FCC (CC = 1.73 kcal mol^{-1}) towards **CB1**, leading to its synergetic energy being 5.00 kcal mol^{-1}, which is fairly in good agreement with its value (4.69 kcal mol^{-1}) in the actual **SW5B** cluster. However, the **CB2** is also common to AC **cycle a** (CC = −0.71 kcal mol^{-1}) and AC **cycle c** (consisting of SO$_2$ and O4, O5, and O6 water molecules) with a small negative CC (−0.86 kcal mol^{-1}). Because of these two AC contributions, **CB2** is the weakest ($E_{CB1}^{Synergetic}$ = 0.46 kcal mol^{-1} and E_{CB1}^{actual} = 0.15 kcal mol^{-1}) bond among all the CBs in the various penta-hydrated clusters studied here. In contrast, the **CB1** bond in the **SW5C** cluster nicely resides at the interface of two FCC tetrameric cycles: **a**
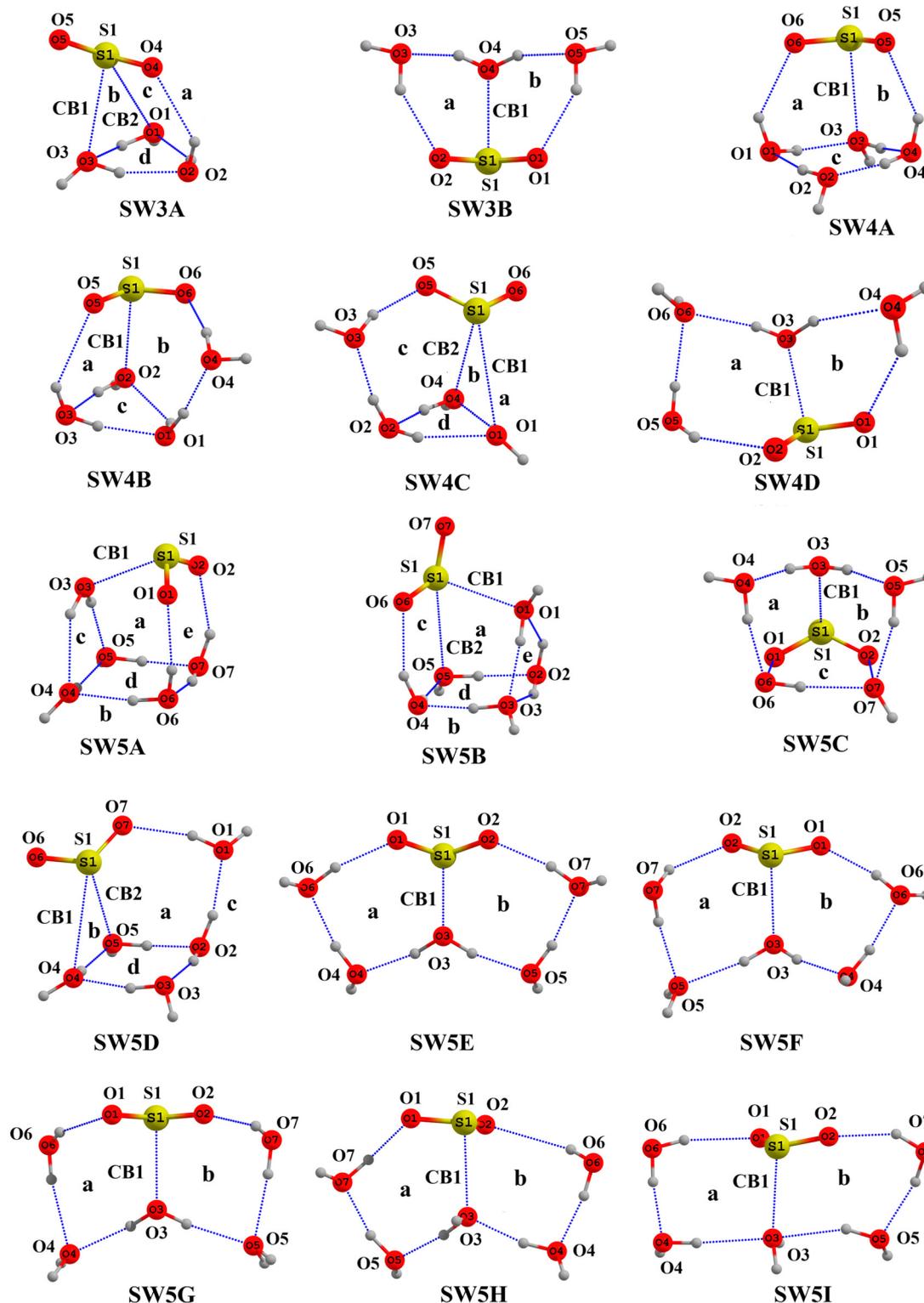
15970 | *Phys. Chem. Chem. Phys.*, 2025, **27**, 15960–15974

This journal is © the Owner Societies 2025

Fig. 4 MP2/6-311++G(d,p) optimized geometries of $SO_2(H_2O)_n$, n = 3–5 clusters.

(consisting of SO_2 and O1, O4, and O6 water molecules) and **b** (consisting of SO_2 and O3, O5, and O7 water molecules). The cooperativity contributions of the two cycles are very large (4.97 and 4.80 kcal mol^{-1}, respectively), making **CB1** the strongest bond

($E_{CB1}^{Synergetic}$ = 11.54 kcal mol^{-1} and E_{CB1}^{actual} = 12.13 kcal mol^{-1}) among all the CBs in the various penta-hydrated clusters studied here. The structure of the **SW5D** cluster is very similar to that of the **SW4C** cluster. The strengths of **CB1** and **CB2** may be similarly explained.

This journal is © the Owner Societies 2025

Phys. Chem. Chem. Phys., 2025, **27**, 15960–15974 | **15971**

Table 3 CB energies (in kcal mol^{-1}) in $SO_2(H_2O)_n$, n = 3 to 5 cluster, along with CB energy in the respective dimer species (E_{CB}^{dimer}). All calculations were performed at the MP2/aug-cc-pVTZ level of theory. See Fig. 4 and the text for details

CB	E_{CB}^{Dimer}	$E_{coop.}^{Cycle1}$	$E_{coop.}^{Cycle2}$	$E_{CB}^{Synergetic}$	E_{CB}^{actual}	$|\Delta E_{CB}|$
SW3A						
CB1	4.11	1.28	−0.38	5.01	4.90	0.11
CB2	0.65	−0.42	−0.38	−0.16	−0.27	0.11
SW3B						
CB1	3.45	2.70	2.69	8.84	8.91	0.07
SW4A						
CB1	3.74	−0.76	1.80	4.78	4.43	0.35
SW4B						
CB1	3.59	1.75	0.09	5.42	5.39	0.03
SW4C						
CB1	0.88	−0.30	−0.46	0.12	−0.003	0.12
CB2	3.52	−0.46	1.84	4.90	4.78	0.12
SW4D						
CB1	3.87	1.10	2.38	7.35	7.37	0.02
SW5A						
CB1	3.91	2.68	0.73	7.32	7.33	0.01
SW5B						
CB1	4.13	−0.86	1.73	5.00	4.69	0.31
CB2	1.40	−0.71	−0.23	0.46	0.15	0.31
SW5C						
CB1	1.77	4.97	4.80	11.54	12.13	0.59
SW5D						
CB1	3.28	1.93	−0.51	4.70	4.48	0.22
CB2	1.02	−0.51	−0.26	0.25	0.08	0.17
SW5E						
CB1	0.53	4.26	4.27	9.06	9.43	0.37
SW5F						
CB1	2.53	1.24	3.00	6.77	6.81	0.04
SW5G[a]						
CB1	2.78	1.46	1.49	5.73	5.74	0.01
SW5H[a]						
CB1	3.08	3.23	−1.26	5.05	4.82	0.23
SW5I[a]						
CB1	3.57	−0.68	−0.62	2.27	2.38	0.11

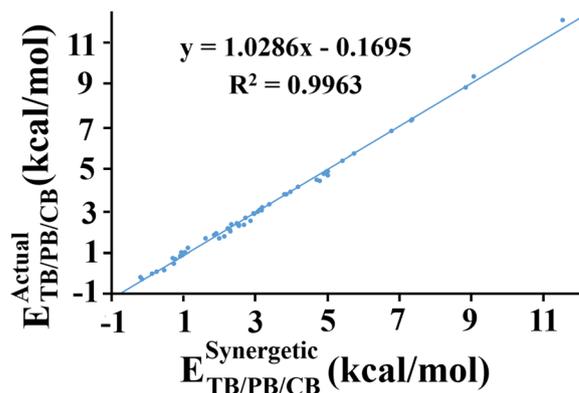[a] Partially optimized.

Fig. 5 Correlation plot between the energy of TB/PB/CB calculated by synergetic cooperativity effects and its value in the actual microhydrated clusters calculated using the MTA-based method.

NW5H, and **NW5I** are partially optimized structures (with certain frozen atoms). Upon full optimization, these structures are not local minima, leading to other structures.

In summary, the proposed method of synergetic cyclic cooperativity can accurately determine the energies of TB, PB, and CBs in various microhydrated clusters of CO_2, N_2O and SO_2, respectively. Fig. 5 shows a correlation plot between the $E_{TB/PB/CB}^{Synergetic}$ versus $E_{TB/PB/CB}^{actual}$ values for all the TBs, PBs and CBs present in various microhydrated clusters of CO_2, N_2O and SO_2 studied in the present work (60 data points). It reveals an excellent linear correlation (R^2 = 0.9963) between these two variables, with the root-mean-square and standard deviation of 0.186 and 0.189 kcal mol^{-1}, respectively. The mean absolute error and maximum absolute errors are 0.11 and 0.59 kcal mol^{-1}, respectively.

Concluding remarks

In this work, the energy of individual non-covalent bonds (NCBs), viz. tetrel (TB), pnictogen (PB) and chalcogen (CBs), which are at the interface of two or more cyclic structures, is estimated using the cooperativity contributions (CCs) of these cycles. The CCs of individual cycles are estimated using the molecular tailoring approach-based (MTA-based) method. The total CCs of all the cyclic structures common to a referenced NCB are added to the energy of this NCB present in a corresponding dimer. Thus, the calculated energy is referred to as the synergetic energy ($E_{NCB}^{Synergetic}$) of NCB. To demonstrate this approach, the microhydrated clusters (up to 5 water molecules) of atmospherically important gases, viz. CO_2, N_2O and SO_2 were taken. In the optimized geometries of these clusters, the water molecule forms TB, PB and CB with C of CO_2, N of N_2O, and S of SO_2, respectively. The energy of such TB, PB and CB common to two or more cyclic structures formed owing to the interconnection of NCBs is evaluated using the proposed method of the synergetic cyclic cooperativity. It has been found that the proposed method also provides very accurate energies of all these NCBs in their respective microhydrated clusters. For instance, the calculated $E_{TB}^{Synergetic}$ values in microhydrated

To further understand the interplay of cyclic cooperativity on the strength of CB, the specially optimized clusters, viz. **SW5E**, **SW5F**, and **SW5G**, were considered, wherein CB is common to two tetrameric **cycles a** and **b**, with different combinations of the nature of cyclic cooperativity. In **SW5E** clusters, these cycles exhibit FCC with CCs being 4.26 and 4.27 kcal mol^{-1}, making **CB1** the strongest bond ($E_{CB1}^{Synergetic}$ = 9.06 kcal mol^{-1} and E_{CB1}^{actual} = 9.43 kcal mol^{-1}) in this class of structures. In **SW5F**, one of these cycles (**cycle a**) is replaced with the one having PCC (CC = 1.24 kcal mol^{-1}), and the strength of **CB1** is moderately decreased ($E_{CB1}^{Synergetic}$ = 6.77 kcal mol^{-1} and E_{CB1}^{actual} = 6.81 kcal mol^{-1}). However, **CB1** strength further weakens ($E_{CB1}^{Synergetic}$ = 5.73 kcal mol^{-1} and E_{CB1}^{actual} = 5.74 kcal mol^{-1}) in the **SW5G** cluster when both cycles exhibit PCC (CCs = 1.46 and 1.49 kcal mol^{-1}). A combination of two cyclic structures in which **cycle a** bears FCC (CC = 3.23 kcal mol^{-1}) and **cycle b** exhibits AC (−1.26 kcal mol^{-1}) leads to further weakening of the **CB1** ($E_{CB1}^{Synergetic}$ = 5.05 kcal mol^{-1} and E_{CB1}^{actual} = 4.82 kcal mol^{-1}) as in **SW5H**. When both **cycles a** and **b** exhibit AC (CC = −0.68 and −0.62 kcal mol^{-1}, respectively), the energy of **CB1** is the smallest in this class ($E_{CB1}^{Synergetic}$ = 2.27 kcal mol^{-1} and E_{CB1}^{actual} = 2.38 kcal mol^{-1}) as in **SW5I**. Note that **NW5G**,

15972 | Phys. Chem. Chem. Phys., 2025, **27**, 15960–15974

This journal is © the Owner Societies 2025

CO_2 clusters fall between -0.21 and 4.98 kcal mol^{-1}, while that for $E_{PB}^{Synergetic}$ values in microhydrated N_2O clusters falls between 0.72 and 3.38 kcal mol^{-1}. The calculated values of $E_{CB}^{Synergetic}$ suggests that the CB bonds in microhydrated clysters of SO_2 could be of very weak to very strong strength (-0.16 to 11.54 kcal mol^{-1}). The qualitative and quantitative strengths of these weak, moderate and strong NCBs are nicely explained in terms of the nature of the cyclic structures to which they are common. For instance, a referenced NCB is common to two or more cyclic structures, both exhibiting full-cyclic cooperativity (FCC), and is found to be the strongest. An NCB is of moderate strength if it is present at the interface of two cyclic structures, of which one exhibits FCC and the other shows partial cyclic cooperativity (PCC). However, NCBs are the weakest if both cyclic structures common to them bear anti-cooperativity (AC).

Most importantly, the calculated energies of these different NCBs (TBs, PBs and CBs) using the method of synergetic cyclic cooperativity are in excellent agreement with the one calculated using the MTA-based method employing the actual microhydrated cluster of these gases ($E_{TB/PB/CB}^{actual}$). For instance, there exists a nice correlation ($R^2 = 0.9963$) between the $E_{TB/PB/CB}^{Synergetic}$ versus $E_{TB/PB/CB}^{actual}$ values for all the NCBs present in various microhydrated clusters of CO_2, N_2O and SO_2. Furthermore, the root-mean-square and standard deviations are 0.186 and 0.189 kcal mol^{-1}, respectively. The mean absolute error and maximum absolute error is 0.11 and 0.59 kcal mol^{-1}, respectively.

In conclusion, the proposed method of the synergetic cyclic cooperativity can accurately estimate the energy of different NCBs, such as HBs, TBs, PBs and CBs, in various microhydrated clusters of atmospherically important gases, thereby proving the general nature of this methodology. In the near future, the applicability of this methodology will be tested on various other NCBs, such as halogen and triel bonds. Currently, the automation of this procedure is underway. Such an automated code in conjunction with our hydrogen bond energy estimation (H-BEE) code[49] would be really useful for rapid evaluation of the energy of NCBs in any large 3D molecular cluster.

Conflicts of interest

There are no conflicts to declare.

Data availability

The data supporting this article have been included as part of the ESI.†

Acknowledgements

References

1 G. Cavallo, P. Metrangolo, R. Milani, T. Pilati, A. Priimagi, G. Resnati and G. Terraneo, *Chem. Rev.*, 2016, **116**, 2478–2601, DOI: 10.1021/acs.chemrev.5b00484.

2 A. C. Legon, *Phys. Chem. Chem. Phys.*, 2017, **19**, 14884–14896, DOI: 10.1039/C7CP02518A.

3 S. Scheiner, *J. Phys. Chem. A*, 2021, **125**, 10419–10427, DOI: 10.1021/acs.jpca.1c09213.

4 A. Varadwaj, P. R. Varadwaj, H. M. Marques and K. Yamashita, *Inorganics*, 2022, **10**, 149, DOI: 10.3390/inorganics10100149.

5 L. Vogel, P. Wonner and S. M. Huber, *Angew. Chem., Int. Ed.*, 2019, **58**, 1880–1891, DOI: 10.1002/anie.201809432.

6 S. Scheiner, *Phys. Chem. Chem. Phys.*, 2021, **23**, 5702–5717, DOI: 10.1039/D1CP00242B.

7 P. R. Varadwaj, A. Varadwaj, H. M. Marques and K. Yamashita, *CrystEngComm*, 2023, **25**, 1411–1423, DOI: 10.1039/D2CE01621D.

8 C. H. Suresh, G. S. Remya and P. K. Anjalikrishna, *Wiley Interdiscip. Rev.: Comput. Mol. Sci.*, 2022, **12**, e1601, DOI: 10.1002/wcms.1601.

9 S. Chandra, B. Suryaprasad, N. Ramanathan and K. Sundararajan, *Phys. Chem. Chem. Phys.*, 2021, **23**, 6286–6297, DOI: 10.1039/D0CP06273A.

10 A. Bauzá, R. Ramis and A. Frontera, *J. Phys. Chem. A*, 2014, **118**, 2827–2834, DOI: 10.1021/jp502301n.

11 S. Scheiner, *CrystEngComm*, 2025, **27**, 921–930, DOI: 10.1039/D4CE01194E.

12 P. Politzer, J. S. Murray and T. Clark, *Phys. Chem. Chem. Phys.*, 2021, **23**, 16458–16468, DOI: 10.1039/D1CP02602J.

13 X. Wang, Q. Li and S. Scheiner, *Phys. Chem. Chem. Phys.*, 2023, **25**, 29738–29746, DOI: 10.1039/d3cp04430k.

14 R. Gupta, S. Singha and D. Mani, *J. Phys. Chem. A*, 2024, **128**, 4605–4622, DOI: 10.1021/acs.jpca.4c00911.

15 N. Liu, Q. Wu, Q. Li and S. Scheiner, *Phys. Chem. Chem. Phys.*, 2022, **24**, 1113–1119, DOI: 10.1039/D1CP05323J.

16 Q. Wu, X. Xie, Q. Li and S. Scheiner, *Phys. Chem. Chem. Phys.*, 2022, **24**, 25895–25903, DOI: 10.1039/D2CP04194D.

17 M. B. Ahirwar, S. R. Gadre and M. M. Deshmukh, *J. Phys. Chem. A*, 2023, **127**, 4394–4406, DOI: 10.1021/acs.jpca.3c00359.

18 D. Patkar, M. B. Ahirwar, S. R. Gadre and M. M. Deshmukh, *J. Phys. Chem. A*, 2021, **125**, 8836–8845, DOI: 10.1021/acs.jpca.1c06478.

19 M. B. Ahirwar, D. Patkar, I. Yadav and M. M. Deshmukh, *Phys. Chem. Chem. Phys.*, 2021, **23**, 17224–17231, DOI: 10.1039/D1CP02839A.

This journal is © the Owner Societies 2025

Phys. Chem. Chem. Phys., 2025, **27**, 15960–15974 | **15973**

20 M. M. Deshmukh, L. J. Bartolotti and S. R. Gadre, *J. Phys. Chem. A*, 2008, **112**, 312–321, DOI: **10.1021/jp076316b**.

21 M. B. Ahirwar, S. R. Gadre and M. M. Deshmukh, *J. Phys. Chem. A*, 2024, **128**, 6099–6115, DOI: **10.1021/acs.jpca.4c01176**.

22 K. Stokely, M. G. Mazza, H. E. Stanley and G. Franzese, *Proc. Natl. Acad. Sci. U. S. A.*, 2010, **107**, 1301–1306, DOI: **10.1073/pnas.0912756107**.

23 S. Blanco, P. Pinacho and J. C. López, *Angew. Chem., Int. Ed.*, 2016, **128**, 9477–9481, DOI: **10.1002/ange.201603319**.

24 A. Sauza de la Vega, T. Rocha-Rinza and J. M. Guevara-Vela, *ChemPhysChem*, 2021, **22**, 1269–1285, DOI: **10.1002/cphc.202000981**.

25 K. J. Tielrooij, N. Garcia-Araez, M. Bonn and H. J. Bakker, *Science*, 2010, **328**, 1006–1009, DOI: **10.1126/science.1183512**.

26 R. P. Sheridan, R. H. Lee, N. Peters and L. C. Allen, *Biopolymers*, 1979, **18**, 2451–2458, DOI: **10.1002/bip.1979.360181006**.

27 J. Li, Y. Wang, J. Chen, Z. Liu, A. Bax and L. Yao, *J. Am. Chem. Soc.*, 2016, **138**, 1824–1827, DOI: **10.1021/jacs.5b13140**.

28 J. M. Guevara-Vela, E. Romero-Montalvo, V. A. M. Gòmez, R. Chávez-Calvillo, M. García-Revilla, E. Francisco, Á. Martín Pendás and T. Rocha-Rinza, *Phys. Chem. Chem. Phys.*, 2016, **18**, 19557–19566, DOI: **10.1039/C6CP00763E**.

29 F. Weinhold, *Molecules*, 2022, **27**, 4218, DOI: **10.3390/molecules27134218**.

30 C. Pérez, D. P. Zaleski, N. A. Seifert, B. Temelso, G. C. Shields, Z. Kisiel and B. H. Pate, *Angew. Chem., Int. Ed.*, 2014, **53**, 14368–14372, DOI: **10.1002/anie.201407447**.

31 O. Mo, M. Yáñez and J. Elguero, *J. Chem. Phys.*, 1992, **97**, 6628–6638, DOI: **10.1063/1.463666**.

32 N. Kobko and J. J. Dannenberg, *J. Phys. Chem. A*, 2003, **107**, 10389–10395, DOI: **10.1021/jp0365209**.

33 A. S. Mahadevi, Y. I. Neela and G. N. Sastry, *Phys. Chem. Chem. Phys.*, 2011, **13**, 15211–15220, DOI: **10.1039/C1CP21346F**.

34 L. Rincon, R. Almeida and D. G. Aldea, *Int. J. Quantum Chem.*, 2005, **102**, 443–453, DOI: **10.1002/qua.20401**.

35 R. F. W. Bader, *Atoms in Molecules: A Quantum Theory*, Clarendon Press, Oxford, 1990.

36 E. Espinosa, E. Molins and C. Lecomte, *Chem. Phys. Lett.*, 1998, **285**, 170–173, DOI: **10.1016/S0009-2614(98)00036-0**.

37 J. M. Guevara-Vela, F. Francisco, T. Rocha-Rinza and A. M. Pendás, *Molecules*, 2020, **25**, 4028, DOI: **10.3390/molecules25174028**.

38 M. M. Deshmukh, S. R. Gadre and L. J. Bartolotti, *J. Phys. Chem. A*, 2006, **110**, 12519–12523, DOI: **10.1021/jp065836o**.

39 M. M. Deshmukh and C. H. Suresh, and S. R, *J. Phys. Chem. A*, 2007, **111**, 6472–6480, DOI: **10.1021/jp071337r**.

40 M. M. Deshmukh and S. R. Gadre, *J. Phys. Chem. A*, 2009, **113**, 7927–7932, DOI: **10.1021/jp9031207**.

41 M. M. Deshmukh, S. R. Gadre and E. M. Cocinero, *New J. Chem.*, 2015, **39**, 9006–9018, DOI: **10.1039/C5NJ02106E**.

42 N. Siddiqui, V. Singh, M. M. Deshmukh and R. Gurunath, *Phys. Chem. Chem. Phys.*, 2015, **17**, 18514–18523, DOI: **10.1039/C5CP02690C**.

43 V. Singh, I. Ibnusaud, S. R. Gadre and M. M. Deshmukh, *New J. Chem.*, 2020, **44**, 5841–5849, DOI: **10.1039/D0NJ00304B**.

44 M. M. Deshmukh and S. R. Gadre, *Molecules*, 2021, **26**, 2928, DOI: **10.3390/molecules26102928**.

45 M. B. Ahirwar, S. R. Gadre and M. M. Deshmukh, *J. Phys. Chem. A*, 2020, **124**, 6699–6706, DOI: **10.1021/acs.jpca.0c05631**.

46 M. B. Ahirwar, N. D. Gurav, S. R. Gadre and M. M. Deshmukh, *Phys. Chem. Chem. Phys.*, 2022, **24**, 15462–15473, DOI: **10.1039/D2CP01663J**.

47 M. B. Ahirwar and M. M. Deshmukh, *J. Phys. Chem. A*, 2023, **127**, 1219–1232, DOI: **10.1021/acs.jpca.2c08087**.

48 M. B. Ahirwar and M. M. Deshmukh, *J. Comput. Chem.*, 2023, **44**, 1861–1874, DOI: **10.1002/jcc.27133**.

49 M. B. Ahirwar, S. S. Khire, S. R. Gadre and M. M. Deshmukh, *J. Comput. Chem.*, 2024, **45**, 274–283, DOI: **10.1002/jcc.27237**.

50 B. Dehariya, M. B. Ahirwar, A. Shivhare and M. M. Deshmukh, *J. Comput. Chem.*, 2025, **46**, e70008, DOI: **10.1002/jcc.70008**.

51 A. Shivhare, B. Dehariya, S. R. Gadre and M. M. Deshmukh, *Phys. Chem. Chem. Phys.*, 2024, **26**, 21332–21336, DOI: **10.1039/D4CP02580F**.

52 A. Shivhare, B. Dehariya, S. R. Gadre and M. M. Deshmukh, *Phys. Chem. Chem. Phys.*, 2025, **27**, 3661–3672, DOI: **10.1039/D4CP04741A**.

53 Z. Rezaei, M. Solimannejad and M. D. Esrafili, *Comput. Theor. Chem.*, 2015, **1074**, 101–106, DOI: **10.1016/j.comptc.2015.10.015**.

54 H. Xu, J. Cheng, X. Yang, Z. Liu, X. Boa and Q. Li, *RSC Adv.*, 2017, **7**, 21713–21720, DOI: **10.1039/C7RA02068F**.

55 S. A. C. McDowell, *Phys. Chem. Chem. Phys.*, 2018, **20**, 18420–18428, DOI: **10.1039/c8cp03641a**.

56 T. M. Ismail, D. Patkar, P. K. Sajith and M. M. Deshmukh, *J. Phys. Chem. A*, 2023, **127**, 10360–10374, DOI: **10.1021/acs.jpca.3c04181**.

57 M. J. Frisch, G. W. Trucks, H. B. Schlegel, G. E. Scuseria, M. A. Robb, J. R. Cheeseman, G. Scalmani, V. Barone, G. A. Petersson and H. Nakatsuji, *et al.*, *Gaussian 16, Revision A.03*, Gaussian, Inc., Wallingford CT, 2016.

15974 | *Phys. Chem. Chem. Phys.*, 2025, **27**, 15960–15974

This journal is © the Owner Societies 2025